Interlamellar amino functionalization of kaolinite

Tunney, James J.; Detellier, Christian

National Research Council Canada   Conseil national de recherches Canada

Canada

Interlamellar amino functionalization of kaolinite

James J. Tunney and Christian Detellier

Abstract: The interlamellar surface of kaolinite has been modified with molecules possessing amino functionalities. Either the dimethyl sulfoxide intercalate of kaolinite (Kao/DMSO) or the *N*-methylformamide intercalate of kaolinite (Kao/NMF) were used as starting materials. One of the products, an ethanolamine functionalized kaolinite (Kao–EOA) was resistant to thermal decomposition in both air and N_2 atmospheres up to temperatures greater than 150°C. Based on results from thermal analysis, IR analysis, ^{13}C CP/MAS NMR spectroscopy, and elemental analysis, a structural model is proposed in which every third interlayer surface hydroxyl group on the aluminol (Al-OH) surface of kaolinite is either replaced with an interlayer $Al-OCH_2CH_2NH_2$ group or is strongly H-bonded to an aminoalcohol molecule. A mixture of both types of linkages could coexist. The amino groups that point away from this surface are each keyed into the $-(SiO-)_6$ macro-rings of the adjacent silicate surface, resulting in an amino-functionalized ordered two-dimensional organo-mineral assembly.

Key words: kaolinite, halloysite, organo-mineral nanocomposites, clay functionalization, supramolecular assemblies.

Résumé : On a modifié la surface interlamellaire de la kaolinite avec des molécules portant des fonctions amino. Comme produits de départ, on a utilisé de la kaolinite intercalée de diméthylsulfoxyde (Kao/DMSO) ou de *N*-méthylformamide (Kao/NMF). Sur l'un des produits, une kaolinite fonctionnalisée à l'éthanolamine (Kao–EAO) est résistante à la décomposition thermique, jusqu'à des températures supérieures à 150°C, dans des atmosphères tant d'air que de N_2. En se basant sur les résultats d'analyses thermiques, d'analyses élémentaires, de spectroscopies IR et RMN ^{13}C avec polarisation croisée/rotation à l'angle magique, «CP/MAS», on propose un modèle structural selon lequel un sur trois groupes hydroxyles de la surface de l'intercouche de l'aluminol (Al-OH) de la kaolinite sont soit remplacés par une intercouche de groupes $Al-OCH_2CH_2NH_2$ soit fortement liés, par liaisons hydrogènes, à une molécule d'aminoalcool. Il est possible que les deux types de liaisons coexistent. Les groupes amino qui sont orientés vers l'extérieur de cette surface sont insérés dans les macrocycles de $-(SiO-)_6$ de la surface adjacente de silicate qui conduit à un arrangement organominéral aminofonctionnalisé ordonné d'une façon bidimensionnelle.

Mots clés : kaolinite, halloysite, nanocomposites organominéraux, fonctionnalisation de l'argile, arrangement supramoléculaires.

[Traduit par la rédaction]

Introduction

It has previously been shown that it is possible to rigidly fix small alcohol moieties onto the interlamellar aluminate surface of kaolinite $(Al_2Si_2O_5(OH)_4)$, through the grafting reaction of the alcohol group to the Al-O-H surface of the kaolinite (1–3). These interesting materials are organo-mineral nanocomposites with organic units covalently attached to the inorganic substrate in an ordered stacking of organo-mineral layers. The non-centrosymmetric kaolinite layers may act as a rigid inorganic supramolecular organizing medium, since the dipole moment that exists across the interlayer space of kaolinite (4–6) may act to orient molecules in a preferred orientation (1–3, 7–16). It would thus be of interest to expand the interlayer grafting chemistry of kaolinite to include other systems than the previously reported alcohol/diol organo-kaolinite system (1–3). It has been demonstrated that despite the slow kinetics of many kaolinite intercalation reactions (8), it is nonetheless possible to intercalate large molecules, such as polyethylene glycol of average molecular weight 3400, into the interlayers of kaolinite by first preswelling with either DMSO or NMF (17). This suggests that kaolinite could be used as a non-centrosymmetric inorganic organizing medium. One may thus envisage rationally assembling sophisticated non-centrosymmetric organo-mineral materials based on rigid inorganic asymmetric kaolinite layers.

With the diol-based organo-kaolinites, the interlayer cohesive forces for these new materials prevented easy layer swelling (1, 2). This was presumably due to the strong hydrogen bonding between the pendant hydroxyl groups of the diols and the silicate surface of the kaolinite layers. As a result, even though the alcohol functionality of the diol unit offers an

J.J. Tunney[1] **and C. Detellier.**[2] Ottawa–Carleton Chemistry Institute, Department of Chemistry, University of Ottawa, Ottawa, ON K1N 6N5, Canada.

[1] Present address: Institute for Chemical Process and Environmental Technology, National Research Council of Canada, Ottawa, ON K1A 0R6. Telephone: (613) 990-2102. Fax: (613) 991-2383. E-mail: Jim.Tunney@nrc.ca
[2] Author to whom correspondence may be addressed. Telephone: (613) 562-5707. Fax: (613) 562-5170. E-mail: dete@science.uottawa.ca

attractive site for further interlayer modification reactions, it is inaccessible to reactant molecules. Other types of organo-kaolinites, preferably with weaker interlayer cohesion and consequently greater swelling properties, are required if one wishes to use them as the first step in the development of more sophisticated structures. Part of the appeal in attaching molecules with pendant amine groups in the interlayer space of kaolinite lies with the possibility of using the free amine group to attach larger molecules to the interlayer surface kaolinite. Amines could, for example, provide an ideal site for the attachment of a carbonyl-functionalized moiety.

Organo-kaolinites with organic guests possessing amino groups have previously been reported. Kaolinite-hydrazine (Kao/Hz) (8, 18–21) is rapidly formed by exposing untreated kaolinite to hydrazine vapours or to a hydrazine solution. Despite its ease of formation, Kao/Hz is much less stable than either Kao/DMSO or Kao/NMF, decomposing in ambient conditions within less than an hour. This ease of formation and inherent instability allows Kao/Hz to be used to advantage as an intermediate in the preparation of other organo-kaolinites via the displacement method (21–23). In related work, Inoue et al. (24) prepared a series of aminoalcohol-based organoboehmite materials in which they proposed that the organic units were attached to the boehmite via $Al-O-(CH_2)_nNH_2$ bonds.

Experimental

Materials

All chemicals used were of reagent grade quality and were not further purified unless otherwise specified. KGa-1, well-crystallized kaolinite, was obtained from the Source Clay Repository of the Clay Mineral Society (Department of Geology, University of Missouri, Columbia, Mo.). Halloysite (coded as Halloysite no. 13 from Eureka, Utah), a polytype of kaolinite, was obtained from Ward's Natural Science Establishment Inc. (Rochester, N.Y.) in the form of hard rocklike chunks. This had to first be ground up to the consistency of a coarse powder before proceeding with the purification procedure. For both kaolinite and halloysite, purification by standard sedimentation procedures to remove the >2 μm size fraction was required (25–27). Even after purification, in the case of kaolinite small amounts of anatase (TiO_2) impurities could be detected by XRD as a sharp weak reflection at $d = 3.52$ Å, corresponding to the (101) reflection of anatase. The purified clays were then characterized by XRD, FTIR, and TGA/DSC, and were found to be consistent with literature data for purified natural kaolinite and halloysite (28, 29).

Characterization

XRD powder patterns were measured on a Philips PW 3710 automated diffractometer using Cu Kα radiation (wavelength = 1.5416 Å). All measurements were taken using a generator voltage of 45 kV and a generator current of 40 mA. A step size of 0.04° 2Θ was used with a dwell time of 0.5 seconds per step. The sample was spun during pattern acquisition, and an automatic divergent slit and a 0.1 mm receiving slit were used without employing any mask. Samples were mounted on a circular glass disk by first dispersing 20–30 mg of sample with 1 mL of methanol, sonicating for 10 s, and allowing the suspension to dry on the glass disk. Some samples were mounted dry by first smearing a small quantity of vaseline to the glass

disk and then placing the powder directly on this. The intercalation ratio (I.R.), which is an indication of the extent of modification, was calculated from the relative intensities of the (001) reflections of the modified organo-kaolinite phase and the unexpanded kaolinite phase (8). The c-spacing or basal spacing is calculated based on the indexed (00*l*) reflections (8). Reflections due to the presence of residual unreacted kaolinite are identified with the symbol K. All *d*-values are given in Ångstrom units (Å), with the relative intensities given in parentheses on a scale where 100 is the intensity of the most intense reflection. The assigned indexing of the reflection is also given in parentheses.

Infrared spectra were obtained on a Bomem Michelson MB 100 FTIR spectrometer using 30–50 averaged scans at 4 cm^{-1} resolution. The samples were prepared as KBr pellets (0.25–0.50% by weight in KBr). X-ray fluorescence (XRF) measurements to measure the Si/Al ratio were performed on a Philips PW 2400 fluorimeter equipped with a Philips PW 2510 sample holder, with the scans referenced to a mixture of SiO_2 and Al_2O_3. Ceramic yields were determined by measuring the residual mass (as a percentage of the starting mass) of the product after calcination at 1100°C for 3 h in air atmosphere. Thermal analyses (TGA and DSC) runs were performed on a Polymer Labs 1500H instrument under either flowing nitrogen or air (20–90 cm^3/min) and a heating rate of 20°C/min. Approximately 10 mg of sample was used for each run using alumina sample and reference pans.

^{13}C cross polarization/magic angle spinning (CP/MAS) spectra (50.33 MHz) were performed on a Bruker ASX-200 instrument with a magic angle spinning rate of 3–4 kHz. The ^{13}C CP/MAS spectra were referenced to hexamethylbenzene at 16.9 ppm. Solution state NMR (^{1}H and ^{13}C) were performed on either a Varian XL-300 or a Bruker AMX-500, and both ^{1}H and ^{13}C chemical shifts are reported relative to TMS in $CDCl_3$.

Starting materials

The preparations of both Kao/DMSO and Kao/NMF and starting materials have been described elsewhere and are based on standard literature procedures (1, 2, 8). Briefly, this involves allowing 20 g of the unexpanded purified kaolinite to remain in contact with DMSO or NMF in an enclosed jar for at least 2 months at room temperature, followed by washing with 1,4-dioxane to remove excess DMSO or NMF, and air drying. After this time, both Kao/DMSO and Kao/NMF are found by XRD to be formed with an intercalation ratio (I.R.) exceeding 90%. XRD patterns, IR spectra, and TGA were all consistent with literature data (8). The DMSO intercalate of halloysite (Hal/DMSO) was formed in an identical manner. In this case, no residual unexpanded halloysite was observed by XRD (8).

Reactions with amines

Kao/DMSO + ethanolamine (Rxn 1)

The reaction of Kao/DMSO with ethanolamine was repeated a number of times and in all cases nearly identical materials resulted. The following is a typical example: 1.0 g of Kao/DMSO (I.R. = 0.97) was refluxed with 50 mL of freshly distilled ethanolamine (EOA) for 22 h under N_2 atmosphere. This was then filtered and washed with 1,4-dioxane to remove excess EOA. Air drying at 40°C for 2 h yielded 0.76 g of an

off-white powder. XRD: 10.64 (100, d_{001}); 7.14 (1.5, d_{001}K); 5.34 (0.1, d_{002}); 4.46 (1.4); 4.34 (2.3); 4.28 (2.1); 4.20 (2.0); 4.15 (1.4); 3.72 (1.2); 3.56 (16.5, d_{003}); 3.32 (0.5); 3.19 (1.2); 3.14 (0.9); 2.84 (0.1); 2.67 (0.7, d_{004}); 2.13 (1.2, d_{005}); 1.78 (0.2, d_{006}); 1.487 (0.3, d_{060}). $d = 10.67 \pm 0.03$ Å, I.R. = 0.985. FTIR (cm^{-1}), ν(O-H): 3693 (s), 3628 (s), 3558 (m), 3486 (s) ν(NH): 3354 (m), 3311 (m); ν(C-H): 3074 (w, br), 2964 (vw), 2946 (w), 2935 (vw), 2889 (w); δ(HOH): 1663 (w); δ(C-H, N-H): 1613 (w), 1525 (w), 1476 (w), 1353 (w), 1197 (w); Si-O vibrations: 1125 (s), 1092 (s), 1045 (vs), 1016 (vs); δ(AlOH): 974 (m), 908 (s); other bands: 2792 (vw), 2691 (w), 2612 (w), 1385 (w, impurity), 874 (w), 796 (w), 740 (w), 683 (m), 604 (w, sh), 552 (s), 471 (s), 433 (s). ^{13}C CP/MAS NMR (Bruker CXP-180, spinning speed = 6 kHz, 45.27 MHz, δ(ppm)): 42 (-CH$_2$NH$_2$), 60 (-CH$_2$O-); no dipolar dephasing signal detected after 40 μs dephasing time for either resonance. Elemental analysis: %C 8.06, %N 4.12; %H 2.72, ceramic yield 72.5%. Calculated for Al$_2$Si$_2$O$_5$(OH)$_{4.0}$(HOCH$_2$CH$_2$NH$_2$)$_{1.0}$: %C 7.52, %N 4.39, %H 3.45, ceramic yield 69.6%. Calculated for Al$_2$Si$_2$O$_5$(OH)$_{3.0}$(OCH$_2$CH$_2$NH$_2$)$_{1.0}$: %C 7.97, %N 4.65, %H 2.99, ceramic yield 73.8%.

Kao/NMF + ethanolamine (Rxn 2)
Kao/NMF (2.0 g) (I.R. = 0.91) was refluxed with 60 mL of ethanolamine (freshly distilled) for 23 h under N$_2$ atmosphere. This was then filtered and washed with 1,4-dioxane to remove excess ethanolamine. Air drying yielded 20 g of an off-white powder. The FTIR and XRD patterns proved to be nearly identical to product (**1**). XRD (vaseline mounted, vacuum dried at 40°C for 3 h): 10.36 (100, d_{001}); 7.02 (3.7, d_{001}K); 4.41 (7.5); 4.31 (9.8); 4.25 (11); 4.15 (9.1); 4.00 (5.6); 3.69 (5.9); 3.53 (23, d_{003}); $d = 10.5 \pm 0.2$ Å; I.R. = 0.96.

Kaolinite + ethanolamine (Rxn 3)
Kaolinite (1.0 g) was refluxed with 50 mL of ethanolamine in a round-bottom flask fitted with a reflux condenser for 17 h under N$_2$ atmosphere. After filtering and washing the reaction mixture with methanol, the product was air dried, yielding 0.9 g of a light grey product. The FTIR pattern of this product was indicative of the well-crystallized kaolinite starting material.

Hal/DMSO + ethanolamine (Rxn 4)
Hal/DMSO (10 g) was refluxed with 40 mL of ethanolamine (freshly distilled) for 20 h under N$_2$ atmosphere. This was then filtered and washed with ethanol to remove excess ethanolamine. Air drying yielded 0.70 g of an off-white powder. XRD: 10.61 (100, d_{001}); 3.55 (13, d_{003}). $d = 10.6 \pm 0.1$ Å; I.R. = 1.0. FTIR (cm^{-1}), ν(O-H): 3695 (s), 3630 (s), 3558 (s), 3491 (s); ν(NH): 3356 (m), 3313 (m); ν(C-H): 3076 (w, br), 2948 (w), 2889 (w); ν(C=O): 1614 (m); δ(C-H, N-H): 1478 (vw), 1355 (vw); Si-O vibrations: 1125 (s), 1035 (vs); δ(AlOH): 908 (s); other bands: 2620 (w), 744 (w), 680 (m), 551 (s), 468 (s), 434 (s).

Kao/DMSO + ethylene diamine (Rxn 5)
Kao/DMSO (1.2 g) (I.R. = 0.97) was refluxed with 60 mL reagent grade ethylene diamine (Aldrich, BP 118°C) in a round-bottom flask fitted with a reflux condenser for 18 h under N$_2$ atmosphere. After filtering and washing the reaction mixture with 1,4-dioxane, the product was air dried, yielding

Table 1. Summary of the organo-kaolinite products formed from the treatment of amines with kaolinite.

Starting material	Reactant	Rxn code[a]	Basal spacing[b] (Å)	I.R.[c]
Kao/DMSO	Ethanolamine	1	10.7	0.98
Kao/NMF	Ethanolamine	2	10.5	0.96
Kaolinite	Ethanolamine	3	NR	
Hal/DMSO	Ethanolamine	4	10.6	1.0
Kao/DMSO	Ethylene diamine	5	NR	
Kao/DMSO	3-Amino-1-propanol	6	11.1	0.58
Kao/DMSO	DL-1-Amino-2-propanol	7	NR	
Kao/DMSO	Nitroaniline	8	NR	

[a]See experimental section for details.
[b]This refers to the basal spacing of the principal modified product phase. NR, no reaction.
[c]Intercalation ratio.

0.8 g of a light grey product. The FTIR pattern of this product was indicative of partially collapsed Kao/DMSO.

Kao/DMSO + 3-amino-1-propanol (Rxn 6)
Kao/DMSO (1.0 g) (I.R. = 0.97) was refluxed with 50 mL of 3-amino-1-propanol (Aldrich, NH$_2$(CH$_2$)$_3$OH, bp 187–188°C) for 19 h under N$_2$ atmosphere. Work-up consisted of cooling, filtering, and washing with methanol; 0.82 g of an off-white powder was recovered after air drying for 1 h. XRD and FTIR patterns were indicative of a partially modified product. XRD: 11.07 (90, d_{001}), 7.10 (66, d_{001}K). I.R. = 0.58. FTIR (cm^{-1}), ν(O-H): 3698 (s), 3652 (m), 3622 (s), 3626 (w, br); ν(NH): 3364 (vw); ν(C-H): 2941 (w), 2878 (w); δ(C-H, N-H): 1574 (w), 1482 (w), 1322 (vw); Si-O vibrations: 1110 (s, sh), 1085 (s), 1046 (vs), 1032 (vs), 1013 (vs); δ(Al-OH): 914 (s); other bands: 791 (w), 752 (w), 685 (m), 539 (s), 472 (s), 431 (s).

Kao/DMSO + DL-1-amino-2-propanol (Rxn 7)
Kao/DMSO (1.0 g) (I.R. = 0.97) was refluxed with 50 mL of DL-1-amino-1-propanol (Aldrich, NH$_2$CH$_2$CH$_2$OHCH$_3$, bp 160°C) for 19 h under N$_2$ atmosphere. Work-up consisted of cooling, filtering, and washing with methanol; 0.72 g of an off-white powder was recovered after air drying for 1 h. FTIR indicated that no modification had occurred, and the Kao/DMSO starting material had reverted to a collapsed kaolinite.

Kao/DMSO + nitroaniline (Rxn 8)
A preliminary attempt to intercalate nitroaniline into the interlayer space of kaolinite was made by reacting 1.0 g of Kao/DMSO in 10 g of melted nitroaniline (mp 149°C) at 175°C for 40 h under N$_2$ atmosphere. During the course of reaction, the mixture slowly turned black. Work-up consisted of repeated washings with methanol to remove as much of the excess organic material as possible. FTIR and XRD patterns were both consistent with a collapsed kaolinite structure.

Results and discussion

Preparation
A series of amines were reacted with Kao/DMSO and Kao/NMF (Table 1). These included the aminoalcohols ethanol-

Fig. 1. XRD pattern (2°–70° 2Θ) for Kao–EOA. K indicates (001) reflection from residual kaolinite.
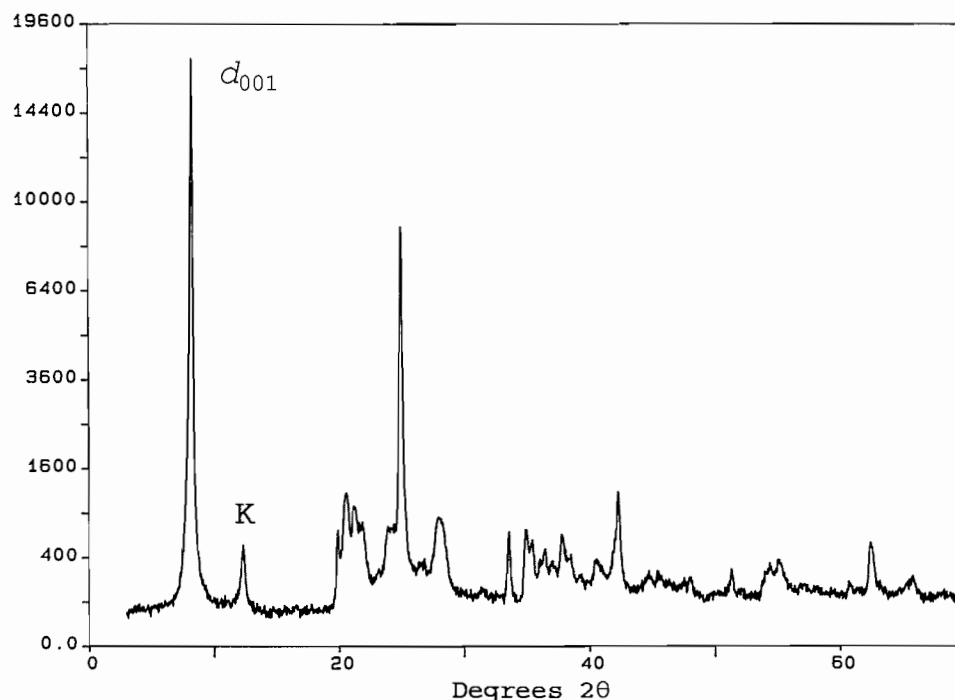
amine (EOA) and 3-amino-1-propanol (3,1-AP), which formed new organo-kaolinite intercalates. The reactions involving ethylene diamine (**5**), DL-1-amino-2-propanol (**7**), and nitroaniline (**8**) were unsuccessful and yielded only collapsed unmodified kaolinite and Kao/DMSO starting material. For Kao–3,1-AP (**6**), the modified phase had a basal spacing of 11.1 Å, and the intercalation ratio (I.R.) was only 0.58. IR results for this material definitely show that the Kao/DMSO starting material has been altered, and one observes bands attributable to the 3-amino-1-propanol guest species. For example, faint ν(NH) bands were detected at 3426 (vw) and 3364 (vw) cm^{-1}, ν(CH) bands at 2941 (w) and 2878 (w) cm^{-1}, and deformation bands at 1574 (w), 1482 (w), and 1322 cm^{-1}. The fact that 3-amino-1-propanol formed an intercalate with kaolinite, whereas DL-1-amino-2-propanol did not, may plausibly be due to the higher reaction temperature for Kao–3,1-AP formation (187°C vs. 160°C), which permitted a more rapid diffusion of 3-amino-1-propanol into the interlayers of kaolinite before structural collapse could occur. Alternately, the presence of an end methyl group in 1-amino-2-propanol may have also made interlayer diffusion more difficult and contributed to a weaker host–guest interaction.

In view of the fact that ethylene diamine may intercalate into halloysite to form an 11.7 Å intercalation complex (30, 31), it is surprising that an organo-kaolinite product was not formed via the displacement of DMSO. Reaction with *para*-nitroaniline was also unsuccessful, presumably due to the hydrophobic nature of *para*-nitroaniline and the weaker basicity of *para*-nitroaniline compared to primary amines.

Clearly, the greatest success was achieved using ethanolamine as the reactant, and this product (Kao–EOA) will be examined in some detail. It was possible to form nearly identical Kao–EOA products from both Kao/DMSO and Kao/NMF starting materials but not from unexpanded kaolin-

ite. This indicates that the intercalating agent (DMSO or NMF) that was used to provide access to the interlamellar space of kaolinite plays a passive role and is not directly involved in the actual chemical reaction between ethanolamine and the interlamellar surface of kaolinite. DMSO and NMF are required only to provide access to the clay interlayers.

The Kao–EOA product exhibited a remarkable crystallinity as exhibited by the strong reflections of the XRD pattern (Fig. 1). The main product had a basal spacing of 10.67 Å. This product was found to be stable with respect to vacuum drying over phosphorus pentoxide for 24 h at 25°C, but was unstable when washed with water overnight, reverting slowly to the parent kaolinite 7.2 Å phase.

It was also possible to form the halloysite analogue of Kao–EOA (Hal–EOA), by reacting Hal/DMSO with ethanolamine (**4**). These materials exhibited similar basal spacings and IR patterns. Hal–EOA was much less crystalline than Kao–EOA, as evidenced by the very broad diffraction peaks. This was presumably due to the turbostratic nature of halloysite and Hal–EOA compared to kaolinite and Kao–EOA. No residual unexpanded parent mineral could be detected for the Hal–EOA, indicating that 100% modification was achieved. This was not the case for Kao–EOA, where a reflection at 7.2 Å representing 1.5% relative intensity indicates the presence of a small amount of residual unexpanded kaolinite.

To our knowledge, an ethanolamine derivative (intercalate or otherwise) of kaolinite has not been previously reported in the literature. Ethanolamine has, however, been reported intercalated in halloysite (31), forming a material with a basal spacing of 10.7 Å, which is similar to what is reported here (**4**). This corresponded to a layer expansion of 3.5 Å, which is less than the 4.0 Å minimum clearance space that was calculated

Fig. 2. IR spectra (3800–2400 cm^{-1}) of Kao–EOA.

Fig. 3. IR spectra (1800–1200 cm^{-1}) of Kao–EOA.
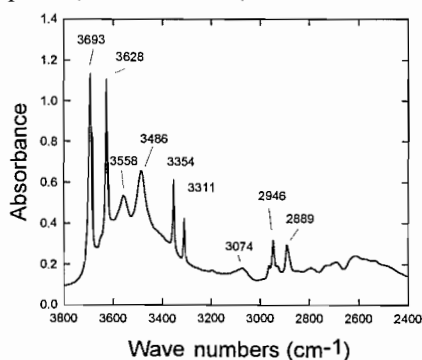
for ethanolamine. This is in accord with many other intercalates that show a smaller than expected basal spacing due to some keying in of the guest (1–3, 8).

IR analysis

The IR patterns of Hal–EOA and Kao–EOA showed strong evidence of modification of the respective host minerals. In particular, the O-H stretching region was greatly perturbed and additional N-H stretching bands could be seen due to the ethanolamine units (Fig. 2). The ν(OH) bands of kaolinite normally found at 3695, 3670, 3652, and 3620 cm^{-1} have been replaced by bands at 3693, 3628, 3558, and 3486 cm^{-1} for Kao–EOA. These last two bands represent significant red shifts, indicating the effects of increased hydrogen bonding between the kaolinite host and ethanolamine guest.

The inner hydroxyl kaolinite peak at 3620 cm^{-1} peak has been blue shifted to 3628 cm^{-1}. A similar blue shift phenomenon for an evacuated (0.01 Torr; 1 Torr = 133.3 Pa) hydrazine intercalated kaolinite was previously attributed to keying of the -NH$_2$ moiety of hydrazine into the siloxane ditrigonal cavity of kaolinite (20). A partial collapse of the hydrazine intercalate from 10.4 to 9.6 Å was associated with this phenomenon. This 8 cm^{-1} shift of the inner hydroxyl ν(OH) band, therefore, provides some evidence for the keying in of the -NH$_2$ group of ethanolamine into the (Si-O-)$_6$ macro-ring of kaolinite. In addition to the O-H stretching region, further evidence for ethanolamine modification includes the presence of two sharp N-H stretching bands at 3354 and 3311 cm^{-1}. C-H stretching bands were observed at 2946 and 2889 cm^{-1} (Fig. 2).

In the deformation region (Fig. 3), an NH bending band at 1613 cm^{-1}, a δ(CH) band at 1476 cm^{-1}, and a C-N stretching band at 1353 cm^{-1} could all be observed. The kaolinite host material also showed signs of perturbation in the lattice vibrations region. The very strong in-plane Si-O-Si stretching vibrations of kaolinite at 1010 and 1033 cm^{-1} (26) are shifted to higher frequencies in Kao–EOA to 1016 and 1045 cm^{-1}. The δ(Al-OH) band of the inner hydroxyl of kaolinite is shifted from 915 to 908 cm^{-1}, and the δ(Al-OH) band of the inner surface kaolinite hydroxyls at 938 cm^{-1} is replaced by a band at 974 cm^{-1}. All this indicates strong host–guest interactions between kaolinite and the ethanolamine moiety.

^{13}C NMR analysis

The solid state ^{13}C CP/MAS NMR spectrum (45.3 MHz) of Kao–EOA showed two broad resonances, one at 43 ppm and
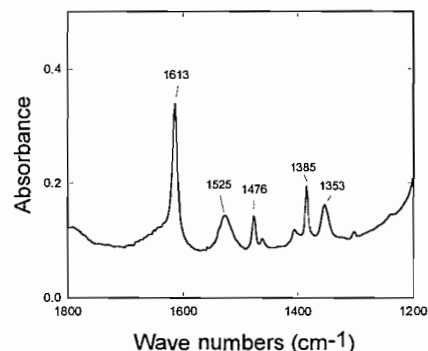
Fig. 4. TGA (20–1200°C) for Kao–EOA. Flowing nitrogen (40 cc/min); the heating rate was 20°C/min.
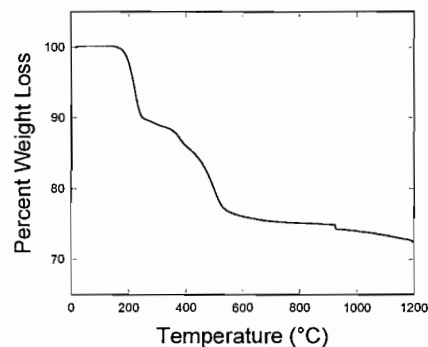

the other at 60.5 ppm corresponding, respectively, to the ^{13}C-NH$_2$ carbon and the ^{13}C-O- carbon of the ethanolamine unit. This was consistent with the insertion of the ethanolamine units in the interlayers of kaolinite. A dipolar dephasing experiment (32) (40 μs interrupted decoupling) led to the complete disappearance of both signals, indicating the existence of a rigidly bound ethanolamine unit, plausibly grafted to the aluminate interlamellar surface via ≡Al-O-CH$_2$CH$_2$-NH$_2$ linkages. Alternatively, the ethanolamine molecule may be intercalated, but held rigidly in place by the inorganic host.

Thermal analysis

Thermal analysis of Kao–EOA shows that decomposition does not occur until about 150°C, and then there appears to be a three-step decomposition ending at 600°C (Fig. 4). The total calcination weight loss after heating to 1100°C in air for 3 h is 27.5%. Hal–EOA differs from Kao–EOA in that there is a preliminary decomposition step (7.6% weight loss) beginning almost immediately upon heating.

The thermal decomposition in nitrogen between 150 and 600°C is characterized by endothermic peaks at 225, 377, and 503°C (Fig. 5a). The peaks at 225 and 377°C are assigned to the endothermic pyrolysis of the interlayer organic material, and the peak at 503°C is assigned to the dehydroxylation of the kaolinite host. In air atmosphere (Fig. 5b), one observes an endothermic peak at 482°C assigned to the dehydroxylation of the kaolinite host material. However, instead of two endothermic events corresponding to the decomposition of interlayer organic material, two exotherms with peaks at 229 and 319°C

Fig. 5. DTA for Kao–EOA under flowing nitrogen (40 cc/min), and flowing air (40 cc/min). The heating rate was 20°C/min.
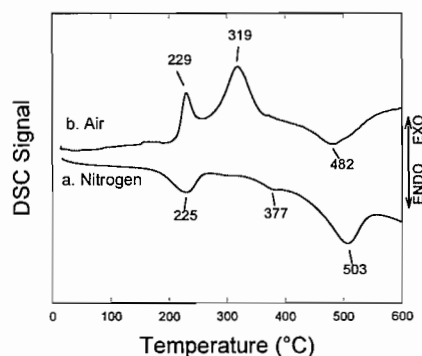
are observed. They are assigned to the exothermic combustion of the interlayer organic material. When the TGA/DSC run was done in air atmosphere, the product after heating to 1100°C was white, indicating that complete combustion of the interlayer organic material had occurred.

Based on elemental analysis of Kao–EOA (**1**), one can assign the formula $Al_2Si_2O_5(OH)_{3.0}(OCH_2CH_2NH_2)_{1.0}$. Here one assumes that grafting has occurred via the condensation reaction of the alcohol group of the ethanolamine with the interlamellar Al-O-H groups of kaolinite. This is consistent with the model for the aminoalcohol-derivatized organoboehmites of Inoue et al. (24) and with the methoxy-functionalized kaolinite (3). There is one ethanolamine unit per $Al_2Si_2O_5(OH)_4$ structural unit of kaolinite, allowing each amino group to key into one $(Si-O-)_6$ macro-ring of the silicate surface of the adjacent layer. Alternately, if one were to consider an ethanolamine unit that is intercalated into the interlamellar surface of kaolinite without grafting, one could assign a chemical formula of $Al_2Si_2O_5(OH)_4(CH_2OHCH_2NH_2)_{1.0}$. The discrepancy between the calculated (3.45%) and found (2.72%) values for the %H of this last assignment suggests that the chemical formula based on the grafting of ethanolamine units $(Al_2Si_2O_5(OH)_{3.0}(OCH_2CH_2NH_2)_{1.0})$ may be a better representation of the structure.

Conclusions

The well-ordered organo-kaolinite material, Kao–EOA, was prepared from the reaction of ethanolamine with both Kao/DMSO and Kao/NMF. A model in agreement with the characterization data can be suggested: an organo-kaolinite material where ethanolamine units are attached to the aluminate interlamellar surface of kaolinite via $\equiv$Al-O-CH_2CH_2NH_2 covalent linkages, with the pendant NH_2 group keyed into the $(SiO-)_6$ macro-ring of the adjacent silicate surface. This model accounts for both the rigidity of the ethanolamine units observed from ^{13}C DD/MAS NMR results, and the relative thermal stability of Kao–EOA. Elemental analysis and IR are also consistent with this structure, representing a supramolecular assembly of dipolar organo-mineral layers, stacked upon each other in an ordered non-centrosymmetric manner. However, on the basis of the basal spacing (10.7 Å) and of the lesser thermal and hydrolytic stability than the corresponding meth-

oxy (3) and ethylene glycol derivatives (2), one can not unambiguously disprove a structure when EOA units would be rigidly intercalated with EOA units keyed into the silicate macro-rings and the aluminol sheets. The prepared material could be a mixture of both types of compounds, intercalated and grafted EOA–kaolinite. A similar mixture could be obtained under certain experimental conditions in the case of the two previously reported ethylene glycol – kaolinite derivatives (1, 2).

Regarding Hal–EOA, the short-range structure of this intercalate appears to be similar to Kao–EOA. The long-range ordering, as evidenced from XRD, indicates that Hal–EOA is arranged in a turbostratic manner whereas Kao–EOA appears to have some three-dimensional ordering. This could be expected on the basis that the parent materials show this same difference in long-range ordering (8, 29).

References

1. J.J. Tunney and C. Detellier. Chem. Mater. **5**, 747 (1993).
2. J.J. Tunney and C. Detellier. Clays Clay Miner. **42**, 552 (1994).
3. J.J. Tunney and C. Detellier. J. Mater. Chem. **6**, 1679 (1996).
4. R.F. Giese. Clays Clay Miner. **26**, 51 (1978).
5. R.F. Giese. Bull. Mineral. **105**, 417 (1982).
6. M. Cruz, H. Jacobs, and J.J. Fripiat. Proc. Int. Clay Conf. 35 (1973).
7. J.A. Raussell-Colom and J.M. Serratosa. *In* Chemistry of clays and clay Minerals. *Edited by* A.C.D. Newman. Mineralogical Society, London. 1987. p. 371.
8. B.K.G. Theng. *In* The chemistry of clay-organo reactions. Adam Hilger, London. 1974. p. 239.
9. S. Hayashi. J. Phys. Chem. **99**, 7120 (1995).
10. M.J. Duer, J. Rocha, and J. Klinowski. J. Am. Chem. Soc. **114**, 6867 (1992).
11. J.G. Thompson and C. Cuff. Clays Clay Miner. **33**, 490 (1985).
12. J.G. Thompson. Clays Clay Miner. **33**, 173 (1985).
13. M. Raupach, P.F. Barron, and J.G. Thompson. Clays Clay Miner. **35**, 208 (1987).
14. S. Olejnik, L.A.G. Aylmore, A.M. Posner, and J.P. Quirk. J. Phys. Chem. **72**, 241 (1968).
15. S. Olejnik, A.M. Posner, and J.P. Quirk. Clay Miner. **8**, 421 (1970).
16. C.T. Johnston, G. Sposito, D.F. Bocian, and R.R. Birge. J. Phys. Chem. **88**, 5959 (1984).
17. J.J. Tunney and C. Detellier. Chem. Mater. **8**, 927 (1996).
18. R.L. Ledoux and J.L. White. J. Colloid. Interface Sci. **21**, 137 (1966).
19. J. Barrios, A. Plançon, M.I. Cruz, and C. Tchoubar. Clays Clay Miner. **25**, 422 (1977).
20. C.T. Johnston and D.A. Stone. Clays Clay Miner. **38**, 121 (1990).
21. A. Weiss, W. Thielepape, G. Göring, W. Ritter, and H. Schäfer. Proc. Int. Clay Conf. 287 (1963).
22. P. Sidheswaran, S.V. Ram Mohan, P. Ganguli, and A.N. Bhat. Indian J. Chem. Sect. A: Inorg. Phys. Theor. Anal. **26A**, 994 (1987).
23. P. Sidheswaran, A.N. Bhat, and P. Ganguli. Clays Clay Miner. **38**, 29 (1990).
24. M. Inoue, H. Tanino, and Y. Kondo. Clays Clay Miner. **39**, 151 (1991).
25. M.L. Jackson, L.D. Whittig, and R.P. Pennington. Soil Sci. Soc. Am. Proc. **14**, 77 (1949).
26. C.B. Tanner and M.L. Jackson. Soil Sci. Soc. Am. Proc. **12**, 60 (1947).

27. R.K. Schofield and H.R. Samson. Discuss. Faraday Soc. **18**, 135 (1954).
28. H. van Olphen and J.J. Fripiat. Data handbook for clay minerals and other non-metallic minerals. Pergamon Press, Oxford. 1979.
29. S.W. Bailey. *In* Crystal structures of clay minerals and their X-ray identification. *Edited by* G.W. Brindley and G. Brown. Mineralogical Society, London. 1984. p. 1.
30. D.M.C. MacEwan. J. Chem. Soc. Faraday Trans. **44**, 349 (1948).
31. R.M. Carr and H.W.A. Chih. Clay Miner. **9**, 153 (1971).
32. L.B. Alemany, D.M. Grant, T.D. Alger, and R.J. Pugmire. J. Am. Chem. Soc. **105**, 6697 (1983).